Food Chemistry 194 (2016) 1245–1253

Contents lists available at ScienceDirect

Food Chemistry

journal homepage: www.elsevier.com/locate/foodchem

Antifreeze and cryoprotective activities of ice-binding collagen peptides from pig skin

Hui Cao, Ying Zhao, Yu Bing Zhu, Fei Xu *, Jing Song Yu, Min Yuan

School of Medical Instrument and Food Engineering, University of Shanghai for Science and Technology, P.O. Box 454, No. 516, Jungong Road, Shanghai 200093, PR China

ARTICLE INFO

Article history:
Received 4 January 2015
Received in revised form 30 July 2015
Accepted 24 August 2015
Available online 28 August 2015

Keywords:
Ice-binding collagen peptides
Thermal hysteresis activity
Crystallisation inhibition activity
Antifreeze protein
Differential scanning calorimetry
Glass transition temperature

ABSTRACT

A novel "hyperactive" ice-binding peptide from porcine collagen was prepared by alkaline protease hydrolysis and a series of column chromatography separations, and then its antifreeze and cryoprotective properties were reported. Using differential scanning calorimetry (DSC), the thermal hysteresis (TH) of ice-binding collagen peptides was closely related to their concentration and crystal fraction. Collagen hydrolysates with maximal TH were obtained by hydrolysis at pH 8.0, DH 15.0%, and 5% alkaline protease at 55 °C. After purification by column chromatography, the AP-3 ice-binding collagen peptide (GLLGPLGPRGLL) with 1162.8 Da molecular weights exhibited the highest TH (5.28 °C), which can be classified as "hyperactive". Recrystallisation and melt-resistance of ice cream were improved by AP-3 ice-binding collagen peptide at 0.2% (w/v) in a similar manner to natural antifreeze proteins. Moreover, the addition of AP-3 collagen peptides in ice cream greatly elevated the glass transition temperature (T_g) to −17.64 °C.

1. Introduction

Antifreeze proteins (AFPs) can bind to ice and inhibit its growth and recrystallisation. Inhibition of ice growth reduces the freezing point (T_0) without changing the melting point (T_m) by a non-colligative mechanism (Kristiansen & Zachariassen, 2008). The resulting difference between freezing and melting points is termed thermal hysteresis (TH). Due to their ice recrystallisation inhibition (*RI*) and TH activities, AFPs can preserve the texture of frozen foods; improve the storage of blood, oranges, and tissues; and protect crops from the freeze–thaw cycle, minimizing or preventing damage to cells and tissues.

AFPs were discovered in 1969 in the blood of the Antarctic fish *Trematomus bernacchii* by DeVries and Wohlschlag (1969). Several other AFPs have subsequently been found in microorganisms (Gilbert, Hill, Dodd, & Laybourn-Parry, 2004), plants (Bravo & Griffith, 2005), insects (Graether & Sykes, 2004) and fish (Fletcher, Hew, & Davies, 2001). These AFPs are structurally diverse and differ considerably in their cryoprotective activities. It has become clear that existing AFPs can be placed in at least two categories based on TH. AFPs from herbaceous and woody plants, TH ranges from 0.06 to 0.35 (Wisniewski et al., 1999; Worrall et al., 1998). Polar-region fishes, where the serum freezing point need only be lowered to just below that of sea water, typically have TH activities of 0.2–0.5 °C at millimolar concentrations. These can be classified as "moderately active" AFPs, including AFP types I, II and III, and antifreeze glycoproteins (Chao et al., 1997; Wua, Banoubb, Goddarda, Kao, & Fletcher, 2001). In contrast, AFPs from many insects have TH activities of 0.6–6 °C at millimolar concentrations (Duman, Bennett, Sformo, Hochstrasser, & Barnes, 2004). Due to their much higher TH at low concentrations, these AFPs are termed "hyperactive".

A distinction between moderate and hyperactive AFPs, aside from the order of magnitude difference in TH, is the way in which they direct ice crystal growth. For moderately active AFPs, ice grows parallel to the *c*-axis, leaving the basal planes unprotected and vulnerable to growth. This is evidenced by "bursts" at the tips of hexagonal bipyramidal ice crystals. For hyperactive AFPs, ice appears to grow along the *a*-axis; the rate of growth along the *a*-axis is ~100 times faster than along the *c*-axis, resulting in a circular disk-like morphology (Pertaya, Marshall, Celik, Davies, & Braslavsky, 2008; Scotter et al., 2006). Clearly, hyperactive AFPs combined with the basal plane give better protection from ice growth by providing more complete ice surface coverage than non-hyperactive AFPs. The ability of hyperactive AFPs to retard recrystallisation and depress the freezing temperature below the melting point suggests potential for utilisation as natural ice modulators in the storage of frozen products (Wang, Agyare, & Damodaran, 2009). However, the limited availability of these

* Corresponding author.
E-mail address: xufei8135@126.com (F. Xu).

http://dx.doi.org/10.1016/j.foodchem.2015.08.102
0308-8146/

natural hyperactive AFPs has restricted their application in the food industry. Thus, there is a need for alternative ingredients to control ice crystal growth during storage of frozen foods.

Recently, Damodaran found that collagen peptides of a certain molecular weight range were able to inhibit recrystallisation of an ice cream mix (Damodaran, 2007). The most prominent feature of collagen peptides is its tripeptide repeat sequence, depicted as -(Gly-Z-X)$_n$-, where X is any amino acid residue and Z always occupied by Pro or Hyp. These repeating units are different from the -Ala-Ala-Thr- sequence found in fish AFGP (Tachibana et al., 2004) but very similar to the Gly-X-X repeating sequences found in two antifreeze proteins from snow fleas (Graham & Davies, 2005). Thus, it is conceivable that the -Gly-Z-X- tripeptide repeat sequences in collagen peptides may play a role in their cryoprotective properties. In the present study, we prepared a novel hyperactive ice-binding collagen peptide from porcine collagen by enzyme hydrolysis and a series of column chromatography separations. Then, we reported its antifreeze and cryoprotective properties in ice cream.

2. Materials and methods

2.1. Materials and chemicals

Porcine skin (age 8–9 months) was provided by Nanjing YuRun Co., Ltd. (Nanjing, China), and stored at −20 °C until use. Alkaline protease (EC 3.4.24., 5 Units/mg) and bovine serum albumin (BSA) were purchased from Sigma Chemical Co (St. Louis, MO, USA). Sephadex G-25 and Sepharose Fast-Flow was provided by Fisher Scientific Co. (Fairlawn, NJ, USA). The composition of the ice cream mix was 8% fat (emulsified), 9% non-fat milk solids, 15.0% sucrose, 0.15% emulsifier and 0.4% stabilizers (carrageenan, guar gum and xanthan gum, 8:85:7). All materials for ice cream preparation were purchased from Sinopharm Chemical Reagent Co., Ltd (SHH, CN). Other chemicals were reagent grade or higher.

2.2. Collagen hydrolysis

Collagen was extracted from porcine skin according to the method of Nagai and Suzuki (2000) and then hydrolysed using alkaline protease to varying degrees of hydrolysis (5%, 10%, 15% and 20%), temperature (45, 50, 55 and 60 °C), pH (7.5, 8.0 and 8.5) and enzyme concentration (2%, 5% and 8%) at a collagen concentration of 15 mg/ml. Afterwards, hydrolysis was stopped by incubating the solution for 5 min in boiling water, and the resulting viscous solution was centrifuged at 4000 r/min for 10 min. The supernatant was lyophilised, and then stored in desiccator placed in a refrigerator (4 °C), until used.

2.3. Determination of the degree of hydrolysis (DH)

The DH [peptide bonds broken (h) as a percentage of total bonds per unit weight (h_{hot})] of collagen hydrolysate was determined using the pH-stat method (Adler-Nissen, 1986) according to the following equation:

$$\mathrm{DH} = \frac{BN_b}{\alpha h_{tot} M_p} \times 100\%$$

where B is the base used in ml; N_b is the normality of the base; α is the average degree of dissociation of the α-NH_2 groups; M_p is the mass of protein in grams (N × 5.95) (Shih & Daigle, 2000); and h_{tot} is the total number of peptide bonds in the protein substrate (7.40 mEq/g rice protein). α was calculated in the following way

$$\alpha = \frac{10^{\mathrm{pH}-pK_a}}{1+10^{\mathrm{pH}-pK_a}}$$

where pH is the value at which enzyme hydrolysis was performed, and pK_a is the average pK_a for α-NH_3^+

2.4. TH determination

The TH of ice-binding collagen peptides was determined using a Pyris Diamond DSC (Perkin Elmer Co., America) (Ding et al., 2014). Temperature and baseline were corrected using naphthalene before all experiments. BSA was used as a standard for AFP-free activity. Briefly, 3.5 μl of sample was injected into the sample cell and quickly frozen by lowering the temperature to −20 °C at a constant rate and then heating to 10 °C at the same rate until totally melted. The enthalpy of melting (H_m) and melting point (T_m) were calculated from the DSC curve. The samples were then repeatedly frozen at −20 °C, followed by slowly heating to a temperature at which the sample was not completely melted, with a certain amount of ice remaining (Φ). To allow for ice-binding collagen peptide interactions with ice and system stabilisation, samples were held at this temperature (T_h, hold temperature) for 15 min before cooling at the same rate to −20 °C, during which the onset temperature (T_0) of crystallisation was recorded and exothermic enthalpy of refreezing (H_r) was calculated. The TH of ice-binding collagen peptides was defined as the difference between T_h and T_0: TH = T_h–T_0. The fraction of ice in the samples was estimated using Φ ($\Phi = (1 - \frac{-\Delta H_r}{\Delta H_m}) \times 100$).

The procedures above were repeated to assess the effects on TH of different heating and cooling rates (1–10 °C/min), hold temperatures (1.3–1.6 °C) and ice-binding collagen peptide concentrations (0.1–30 mg/ml).

2.5. Isolation of ice-binding collagen peptides

Collagen hydrolysates (3 ml, 10 mg/ml) were loaded onto a Sepharose Fast-Flow column (3.5 × 30 cm), which had been equilibrated previously with 50 mM Tris–HCl buffer (pH 8.0) at a flow rate of 2 ml/min. Unbound protein was washed out with 50 mM Tris–HCl buffer (pH 8.0). Retained protein was eluted using a linear gradient of 0.5–1.5 M NaCl in the same buffer. The elution profile was determined by measuring the absorbance at 220 nm. Tubes corresponding to each fraction were pooled separately, desalted and lyophilised and their THA was determined.

The most active fraction (3 ml, 5 mg/ml) was subsequently loaded onto a Sephadex G-25 gel-filtration column (1.5 × 100 cm) and eluted with distilled water. The flow rate was maintained at 0.5 ml/min and the absorbance of elution profile was determined at 220 nm. Tubes corresponding to each fraction were pooled and lyophilised and their THA was determined.

After gel filtration chromatography, fractions that showed the highest TH activity were loaded onto a C18 column (10 × 250 mm). The HPLC system (Waters Company, Milford, Massachusetts, USA) was operated at a flow rate of 3 ml/min at room temperature and the UV detector was set at 220 nm. The column was equilibrated with 5% acetonitrile for 5 min after injection, then the peptides were eluted in succession by a linear gradient of 5–65% acetonitrile solution for 20 min and a linear gradient of 65–100% acetonitrile solution for 2 min. High absorbance fractions were collected and TH activity was determined.

2.6. Peptide sequence analysis by UPLC–ESI-TOF/MS

Ice-binding collagen peptide with the highest TH activity were characterised using an ultra performance liquid chromatography–positive ion electrospray-time of flight mass spectrometer (UPLC–ESI-TOF/MS, Waters Company, Milford, Massachusetts, USA). The peptide sequence was analysed using a Waters SYNAPT

Q-TOF MS system and the De Novo Explorer software. The parameters for the analysis were as follows: reflector, positive; mass range, 20–1500 m/z; ESI source temperature, 100 °C; desolvation temperature, 400 °C; capillary voltage, 3.5 kV; photomultiplier tube voltage, 1800 V.

2.7. Cryoprotective activities of ice-binding collagen peptide in ice cream

2.7.1. Preparation of ice cream samples

Ice cream mixes (8% fat, 9% non-fat milk solids, 15% solid sweetener, 0.15% emulsifier and 0.4% stabilizers) were pasteurised at 76 °C for 15 min using a water bath. Two-stage homogenisation was carried out at 13 MPa in the first stage and 3.4 MPa in the second stage to form tiny fat globules. The ice cream mixes were rapidly cooled at 4 °C and remained at constant temperature for 18 h to age.

2.7.2. Determination of the glass transition temperature (T_g) of ice cream

The glass transition temperature of ice cream was determined using a Pyris Diamond DSC (Perkin Elmer Co., American). Briefly, aliquots (15 mg) of each sample were sealed in aluminium pans and placed in the DSC. The samples were quickly frozen by reducing the temperature to −50 °C at 10 °C/min and held for 15 min at this temperature. The temperature was then gradually increased from −50 to 15 °C at 1 °C/min and held for 15 min. T_g was calculated by constructing tangents to the DSC curve baselines before and after the glass transition. 0.5% BSA was used as a standard for AFP-free activity.

2.7.3. Recrystallisation inhibition (RI) activity of ice-binding collagen peptide

RI activity of ice-binding collagen peptides in ice cream was determined using a cold stage (Model THMS600, Linkham Scientific Instruments, Ltd., Surrey, UK) mounted on a U-TV0.63C microscope (Olympus Co., Isigawakenn, JP). In a typical experiment, a small drop (5 μl) of ice cream (with or without collagen peptides) was placed on a glass microscope slide and covered with a glass coverslip. The slide was placed inside the chamber of the cooling stage and quickly frozen by decreasing the temperature to −50 °C at 20 °C/min. After being held at −50 °C for 15 min, the temperature was gradually increased from −50 to −16 °C at 1 °C/min and cycled between −16 and −14 °C at 1 cycle/3 min. A minimum of 7 cycles was employed, and microscopic images of the sample were then recorded at 40× magnification.

2.7.4. Air bubble assays in ice cream

The size and shape of air bubbles in ice cream were measured using a cold stage mounted on a U-TV0.63C microscope. A small drop (5 μl) of ice cream (with or without ice-binding collagen peptides) was placed on a glass microscope slide and covered with a glass cover slip. The slide was placed inside the chamber of the cooling stage and quickly frozen by decreasing the temperature to 10 °C at 20 °C/min. Microscopic images of the sample were recorded at 40× magnification.

2.7.5. Melting resistance of ice cream

Melting tests were conducted according to the method of Muse and Hartel (2004). Ice cream samples (100 g) were placed on a wire screen (6 holes/cm) on top of a funnel attached to a graduated cylinder. The samples were left to melt in controlled temperature chambers at 37 °C, and the volume melted was recorded at scheduled time intervals. Melting behaviour was defined as the ratio of the melted volume of ice cream after 37 °C treatment to the initial volume.

2.8. Statistical analysis

Data were expressed as the mean ± SD. Statistical significance was determined by one-way analysis of variance with Dunnett's post hoc test using SPSS 13.0 software. P-values less than 0.05 were considered to be significant.

3. Results and discussion

3.1. Conditions for determination of TH activity

Thermal hysteresis is defined as the difference between the melting point and the non-equilibrium freezing point of a solution and is used as an indicator of AFPs activity. At present, TH is commonly measured by direct microscopic observation of crystal growth (Ding et al., 2014). The ice fraction in the sample is approximately estimated according to the radii of the observed crystals, based on the assumption that the ice crystals are of ideal form. Apparently, this method is observer-dependent and cannot accurately quantify ice fraction, due to differences between real and ideal crystals. In this study, to obtain hyperactive ice-binding collagen peptides and accurately assess their antifreeze activity, a DSC method of high simplicity, sensitivity and stability was selected to determine the TH activity of collagen peptides.

In the DSC method, frozen ice-binding collagen peptides samples of 30 mg/ml, which was prepared with enzyme concentrations of 5%, pH 8.0, and a DH of 10% at 55 °C, were first heated to melt partially at a hold temperature of 1.5 °C. Recrystallisation of partially melted ice-binding collagen peptides started immediately after the temperature was reduced. The resulting DSC curves and corresponding data for ice-binding collagen peptides with variable heating and cooling rates were presented in Fig. 1B and E. Compared with the DSC data for BSA (Fig. 1A), the exothermic peaks of ice-binding collagen peptides were delayed significantly ($P < 0.05$), suggesting that the collagen peptides caused thermal hysteresis. Maximal TH was observed with a delay in the exothermic onset of 2.93 °C at heating and cooling rates of 1 °C/min, but no significant discrepancy was found at different heating and cooling rates ($P > 0.05$).

The effect of hold temperature on the TH of ice-binding collagen peptides was also investigated by maintaining heating and cooling rates of 1 °C/min at a collagen peptide concentration of 30 mg/ml. As reported previously, a linear and negative relationship between TH and the ice crystal fraction was found (Hansen & Baust, 1988; Lu et al., 2002; Ramlov, DeVries, & Wilson, 2005). When T_h was within the range of 1.3–1.4 °C and the proportion of ice nuclei (ϕ) in the equilibrium sample was greater than 10%, the recrystallisation of partially melted collagen peptides was delayed slightly as the temperature dropped (Fig. 1C and E). When the proportion of ice nuclei was further decreased to approximately 5%, a larger delay in the onset of refreezing was observed, with a maximum of 4.74 °C; exothermic peaks appeared in a smoother manner. The loss of TH with increasing ice fraction may be linked to a change of adsorption concentration for ice-binding collagen peptides onto the crystal surface during TH measurement (Baardsnes & Davies, 2002; Desjardins, Le Francois, Fletcher, & Blier, 2007). As the ice fraction increased, the increase in ice surface area was much greater than the increase in the concentration of ice-binding collagen peptides in the liquid. The great increase in ice surface area, to which ice-binding collagen peptides are thought to be adsorbed, resulted in a substantial increase in average distance between adjacent collagen molecules on the ice surface (Hansen & Baust, 1988). This implies that the final equilibrium density of ice-binding collagen peptides on the ice surface was smaller than expected from the initial concentration, leading to a reduction in hysteresis.

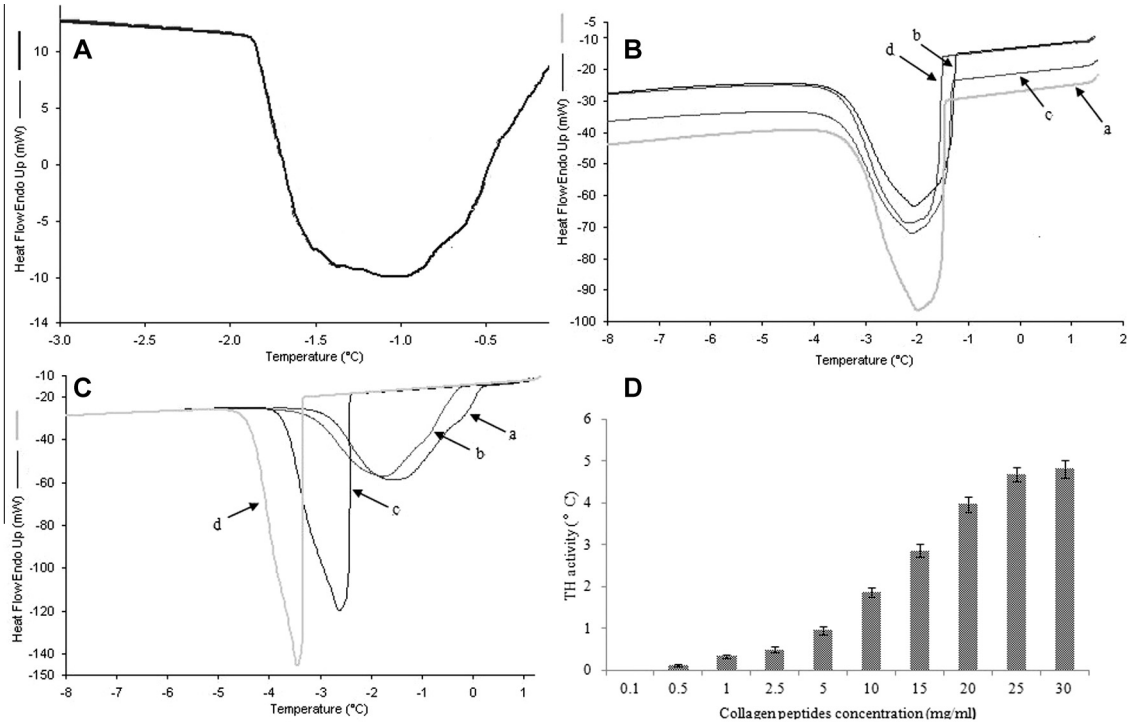

E	Heating and cooling rate (°C/min)				Hold temperature (°C)				BSA
	a	b	c	d	a	b	c	d	
T_h/ °C	1.5	1.5	1.5	1.5	1.3	1.4	1.5	1.6	-0.08
T_0/ °C	-1.43	-1.26	-1.32	-1.19	0.19	-0.34	-1.82	-3.14	-0.09
$\triangle H_r$/J	-232.36	-230.84	-231.60	-231.51	-204.53	-209.77	-231.33	-243.00	-244.35
ϕ%	10.0	10.3	10.2	10.1	20.6	18.5	10.2	5.4	5.2
THA/ °C	2.93	2.76	2. 82	2.69	1.11	1.74	3.32	4.74	0.01

Fig. 1. Effects of heating and cooling rates (B), hold temperature (C) and ice-binding collagen peptide concentration (D) on TH with BSA as the reference (A). In (B), heating and cooling rates were 1 °C/min (a), 2.5 °C/min (b), 5 °C/min (c) and 10 °C/min (d); in (C), hold temperatures were 1.3 °C (a), 1.4 °C (b), 1.5 °C (c) and 1.6 °C (d); (E) hold and onset temperature (T_h and T_0), recrystallisation enthalpy, ice fraction and TH of ice-binding collagen peptides at different hold temperatures and heating and cooling rates, with BSA as the reference.

According to the widely accepted adsorption-inhibition mechanism (Raymond & DeVries, 1977), a plateau of TH is reached when the ice surface is saturated with AFPs. We found that TH for dilute ice-binding collagen peptides was conspicuously low; hysteresis vanished completely below a threshold concentration of ~0.5 mg/ml. Above the threshold, TH increased gradually with ice-binding collagen peptide concentration. The TH of ice-binding collagen peptides reached a maximum at 30 mg/ml, with a 4.82 °C freezing point depression (Fig. 1D). The reason for this finding is unclear, but one possible explanation is that cooperative interactions between ice-binding collagen peptides on the ice surface are required for complete inhibition of crystal growth. At low concentrations, binding between ice-binding collagen peptides and ice crystals (mainly individual interactions) is reversible and weak, leading to a reduction of complementarity to the ice surface and a large drop in TH. Above a critical concentration, ice-binding collagen peptides begin to bind cooperatively through side-by-side hydrophobic interactions, resulting in more efficient adsorption to the ice surface. This increases the coverage of the ice surface, forcing crystal growth into more highly curved fronts, and TH is then observed (Wen & Laursen, 1992). Accordingly, when the ice surface is completely covered by ice-binding collagen peptides, TH no longer increases. Burcham et al. explained the nonlinear correlation between antifreeze activity and AFPs concentration as a consequence of saturation dynamics at the ice surface (Burcham, Osuga, Yeh, & Feeney, 1986).

3.2. Preparation of collagen hydrolysates with higher TH activity

The products of collagen hydrolysis by alkaline protease are generally peptides with a range of molecular weights. Due to the relevance of peptide functionality and molecular size, several parameters were tested to obtain collagen hydrolysates with maximal TH. The results are summarised in Fig. 2.

As shown in Fig. 2, hydrolysis temperature, alkaline protease concentration and DH had a significant effect on the TH of collagen hydrolysates ($P < 0.05$), but pH did not ($P > 0.05$). Only a slight change in TH occurred when pH was increased from 7.5 to 8.5 (Fig. 2c). At 55 °C, the collagen hydrolysates had a higher TH (3.24 °C) with pH 7.5, DH 10.0% and 5% alkaline protease concentration (Fig. 2a). When the alkaline protease concentration was increased to 8% with the other conditions held constant, no significant difference was found at 5–8% enzyme concentration ($P > 0.05$), suggesting that the alkaline protease became saturated

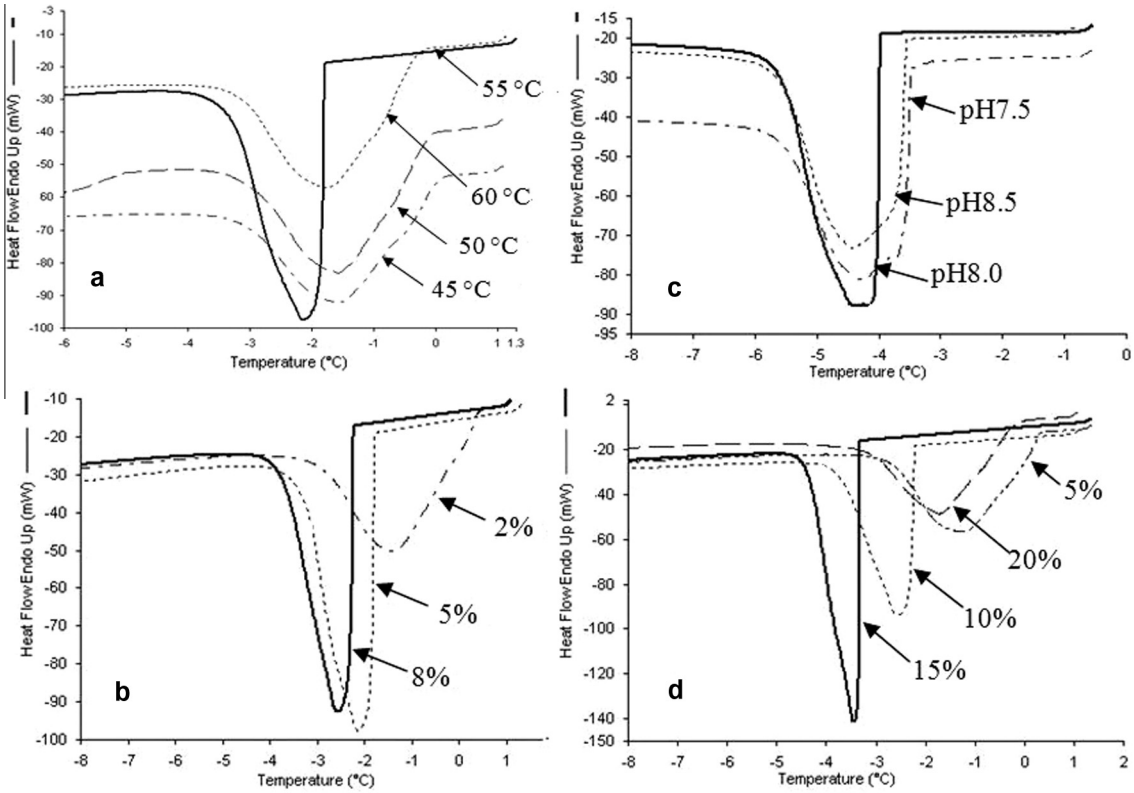

Fig. 2. Effects of hydrolysis temperature (a), alkaline protease concentration (b), pH (c) and DH (d) on TH of collagen hydrolysates. Hydrolysis conditions were pH 7.5, DH 10.0% and alkaline protease concentration 5% at 45–60 °C (a); pH 7.5, DH 10.0% and alkaline protease concentration 2–8% at 55 °C (b); pH 7.5–8.5, DH 10.0% and alkaline protease concentration 5% at 55 °C (c); and pH 8.0, DH 5–20.0% and alkaline protease concentration 5% at 55 °C (d).

in 15 mg/ml collagen (Fig. 2b). The TH of collagen hydrolysates was strongly dependent on DH (Fig. 2d). At relatively low DH (5%), TH was not more than 0.98 °C at pH 8, alkaline protease concentration 5% and 55 °C. As DH increased from 10% to 15%, TH increased from 3.32 to 4.69 °C. However, a further increase in DH from 15% to 20% resulted in a significant decrease in TH ($P < 0.01$). It seems, therefore, that collagen hydrolysates with higher TH can be obtained at pH 8.0, DH 10.0%, alkaline protease concentration 5% and temperature 55 °C.

3.3. Isolation of hyperactive ice-binding collagen peptides

The collagen hydrolysates were first loaded onto an anionic exchange chromatography column of Sepharose Fast-Flow. It appeared three fractions, unadsorbed cationic peptides termed P_1 and P_2 fractions and adsorbed anionic peptides that were eluted by the 0.5–1.5 M NaCl gradient termed P_3 fraction (Fig. 3a). It can be noted that the TH of unadsorbed fraction (P_1) which mainly contained cationic peptides was higher than the adsorbed fraction (P_3), and the TH was 4.21 °C (Fig. 3b). P_1 fraction was pooled, lyophilised and then loaded onto a Sephadex G-25 gel filtration column, the elution profile was as shown in Fig. 3c. It was indicated that P_1 was separated to four fractions: $P_{1\text{-}1}$, $P_{1\text{-}2}$, $P_{1\text{-}3}$ and $P_{1\text{-}4}$. As the temperature fell, the recrystallisation of partially melted $P_{1\text{-}1}$, $P_{1\text{-}2}$ and $P_{1\text{-}4}$ was only delayed slightly. In contrast, a longer delay in the onset of refreezing for $P_{1\text{-}3}$ was observed, with a maximal TH of 4.86 °C (Fig. 3d). $P_{1\text{-}3}$ fraction was subsequently loaded on to a C18 reversed phase high performance liquid chromatography column (Fig. 3e). Three major fractions exhibited TH activity, the highest of which (5.28 °C) was in AP-3 (Fig. 3f). Compared with TH values of 0.2–0.5 for moderate antifreeze proteins (Chao et al., 1997; Wisniewski et al., 1999; Wua et al., 2001), the TH of AP-3 ice-binding collagen peptide was higher, similar to AFPs from insects and fish, such that the AP-3 can be classified as "hyperactive".

3.4. Primary structure of the AP-3 ice-binding collagen peptide

The peptide sequence of AP-3 fraction that demonstrated strong antifreeze activity was analysed by UPLC–ESI-TOF/MS. Fig. 4 shows a typical mass spectrum of AP-3 fraction obtained from TOF-MS analysis with positive ion mode (ESI+). AP-3 fraction had the highest abundance and highest resolution of all the ions with a molecular mass of 1162.80 Da (Fig. 4a). A clean MS spectrum was obtained from AP-3 fraction, and some a-, b- and y-ions derived from the peptide ion are also shown in Fig. 4b. De Novo Explorer software and the electrospray ionisation-principles and practice, demonstrated that AP-3 peptide ion was inferred to be GLLGPLGPRGLL. It could be found that the AP-3 sequence was periodically repeated by Gly-Z-X tripeptide and most of Z was proline. As we all know, the most prominent feature of collagen is its tripeptide repeat sequence, depicted as $-(\text{Gly-Z-X})_n-$, where X is any amino acid residue. Meanwhile, collagen averagely contains 33% Gly and 33% Pro or Hyp, thus the second position in this tripeptide repeat is more often occupied by Pro or Hyp (Gelse, Poschl, & Aigner, 2003). Therefore, the amino acid composition of AP-3 deduced by sequence analysis was in excellent agreement with structure properties of the natural collagen.

Other Gly-rich antifreeze proteins have also been studied and the result revealed that most of these resemble antifreeze proteins were found to be derived from microorganism and insects, such as *Xanthomonas, Brucella, Silicibacter lacuscaerulensis*, snow flea, and so on (Lin, Graham, Campbell, & Davies, 2007; Wang, Zhao, Chen, Zhou, & Wu, 2014). Among these, the peptide fragment sequence

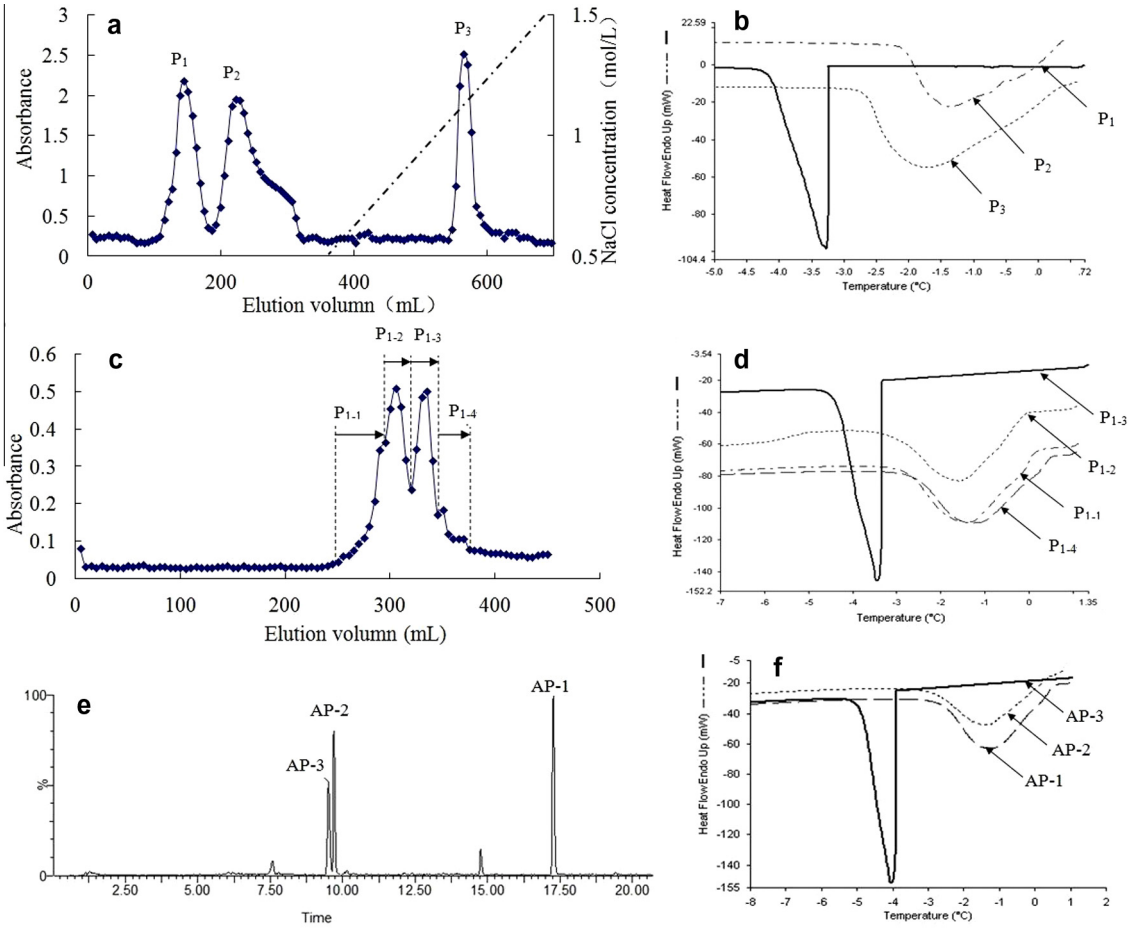

Fig. 3. Purification diagrams and DSC curves of ice-binding collagen peptides. (a) Elution profile of collagen hydrolysates on a Sepharose Fast-Flow chromatographic column; (b) DSC curves of fractions (P_1–P_3) eluted from Sepharose Fast-Flow chromatographic column; (c) elution profile of P_1 fraction on a Sephadex G-25 gel-filtration chromatographic column; (d) DSC curves of fractions (P_{1-1}–P_{1-4}) eluted from Sephadex G-25 gel-filtration chromatographic column; (e) elution profile of P_{1-3} fraction on a C18 column; (f) DSC curves of fractions (AP-1, AP-2 and AP-3) eluted from C18 column.

(GAAGAGSSGP) from snow flea antifreeze protein had the highest sequence similarity with the AP-3 ice-binding collagen peptide. Wang et al. obtained Gly-rich antifreeze peptides (GAIGPAGPLGP) from shark skin. Interestingly, this Gly-rich tripeptide repeat sequence (Gly-Z-X-) of shark skin antifreeze protein which provided a very high degree of molecular flexibility to making hydrogen bonds or Gly-rich faces, was strikingly similar with the AP-3 ice-binding collagen peptide (Wang et al., 2014; Wu et al., 2015). These results revealed the fact that this type of peptide fragment structure have played important role in the antifreeze activity of some AFPs.

3.5. Cryoprotection by AP-3 ice-binding collagen peptide in ice cream

Ice cream is a very temperature-sensitive product: temperature variations during storage and distribution may reduce the quality because of recrystallisation. To improve the robustness of ice cream to storage and transportation, AP-3 ice-binding collagen peptide was added in ice cream and their cryoprotection activity assayed.

3.5.1. Glass transition temperature (T_g) and RI activity of AP-3 ice-binding collagen peptide in ice cream

The determination of T_g is of critical importance in ice cream products, as it is strongly associated with their thermodynamic stability during storage. To prevent recrystallisation, ice cream is best preserved in a glassy state at −30 to −40 °C, but in a typical household freezer, where the temperature is typically above −20 °C and fluctuates widely. Therefore, AP-3 ice-binding collagen peptide was added to control the transition from highly viscous and rubbery to the glassy state and to inhibit ice crystal growth. As shown in Fig. 5H, compared with the blank and BSA groups, addition of less than 0.1% (w/v) AP-3 ice-binding collagen peptide to ice cream caused a slight elevation of T_g ($p > 0.05$) from −31.69 to −29.34 °C. When the concentration of AP-3 ice-binding collagen peptide was higher than 0.1% (w/v), a significant increase in glass temperatures ($p < 0.05$) was observed, with a maximum of −17.64 °C. This suggests that ice cream could be stored in the glassy state in a household freezer and that ice crystal growth may be inhibited.

Ice cream is a complex frozen colloidal system consisting of partially coalesced fat droplets, air bubbles, ice crystals and a cryo-concentrated aqueous phase (Li, Marshall, Heymann, & Fernando, 1997). Due to the thermodynamic instability of ice cream, recrystallisation occurs during storage, leading to a gradual increase in ice crystal mean size and deterioration of product quality (Regand & Goff, 2002). Therefore, the splat assay was used with a minor modification to analyse the *RI* of AP-3 ice-binding collagen peptide in ice cream. Fig. 5 shows the effects of different concentrations of AP-3 ice-binding collagen peptide on crystal growth in ice cream mix after seven cycles between −14 and −16 °C. Recrystallisation was not inhibited by collagen peptides below 0.05% (w/v), where the size

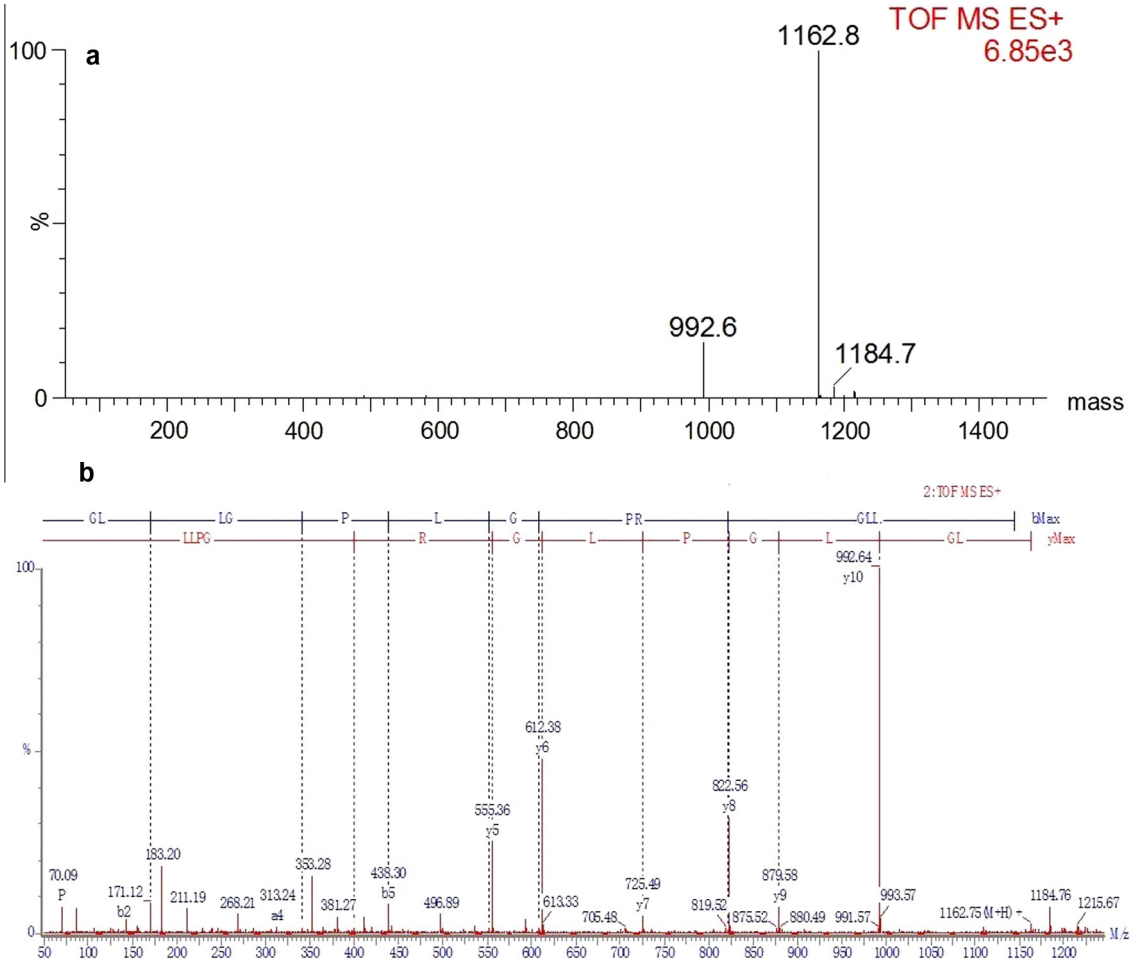

Fig. 4. The molecular weight of AP-3 fraction analysed by UPLC–ESI-TOF-MS (a); MS spectrum of the AP-3 fraction analysed by UPLC–ESI-TOF-MS in positive ion mode, and some a-, b- and y-ions derived from the peptide ion are also shown.

and shape of ice crystals after seven thermal cycles was similar to that of the control mix. In contrast, concentrations over 0.1% (w/v) inhibited ice crystal growth and remarkable *RI* was observed at 0.5% (w/v).

It can be concluded from the above that above 0.1% (w/v), recrystallisation was inhibited. It is generally assumed that AFPs cause *RI* by adsorption to the ice surface and that this adsorption event requires an almost perfect structural match between the ice-binding residues within the binding site of the AFPs and the oxygen atoms at the ice surface (Kristiansen & Zachariassen, 2008; Raymond & DeVries, 1977). Damodaran has analysed several similar collagen peptide models, often depicted as -(Gly-Z-X)$_n$-, using ChemSite Pro molecular modelling software (Damodaran, 2007). There, peptides sequences with small amino acid residues (such as Ala, Ser, Pro and Gly) invariably exhibited an oxygen triad plane (flat face) at the C-terminus with two O–O distances of approximately 4.538 Å. This distance is very close to the 4.52 Å found in the prism face of ice nuclei (Holt, 2003; Yeh & Feeney, 1996). In our study, the peptides sequence of AP-3 fraction was periodically repeated by Gly-Z-X tripeptide and most of sequence was small amino acid residues. Thus, binding of this oxygen triad plane to the prism face of ice nuclei via hydrogen bonding appears to be the mechanism by which AP-3 ice-binding collagen peptide inhibit ice crystal growth. In addition, the aliphatic side chains of Leu and Pro residues in AP-3 ice-binding collagen peptides may provide a partially nonpolar environment to stabilize such hydrogen bonding interactions against competition from ice-water hydrogen bonding interactions (Wang & Damodaran, 2009). Furthermore, collagen peptides with molecular weights of over 1000 Da may be able to form stiff collagen-type helical rods, which may favour stacking of these rods on ice nuclei, with the oxygen triad plane facing the prism face of ice nuclei (Damodaran, 2007). On the other hand, collagen peptides under 1000 Da may lose stiffness, and as a result, steric hindrance may prevent proper stacking of the peptides on the prism face of ice nuclei, thus decreasing their ability to inhibit ice crystal growth.

3.5.2. Melting characteristics

The melting ratio of ice cream is affected by many factors, including ingredients, the consistency coefficient of the mix, the amount of air incorporated, the nature of the ice crystals, and the network of fat globules formed during freezing. Muse and Hartel (2004) found that the melting rate of ice cream increased with storage time, which may be due to increased crystal size as a result of recrystallisation. AP-3 ice-binding collagen peptide, due to their antifreeze activity, significantly reduced the recrystallisation of ice cream. We therefore also investigated the melting resistance of ice cream.

Fig. 6 shows the melting behaviour of ice cream with or without added AP-3 ice-binding collagen peptide. Compared with control and BSA groups, AP-3 ice-binding collagen peptide (0.05% and 0.1%) only slightly improved the melting rate with increasing treatment time. However, as AP-3 concentration was increased to 0.3%, the ice cream started to melt approximately 8 min later at 37 °C,

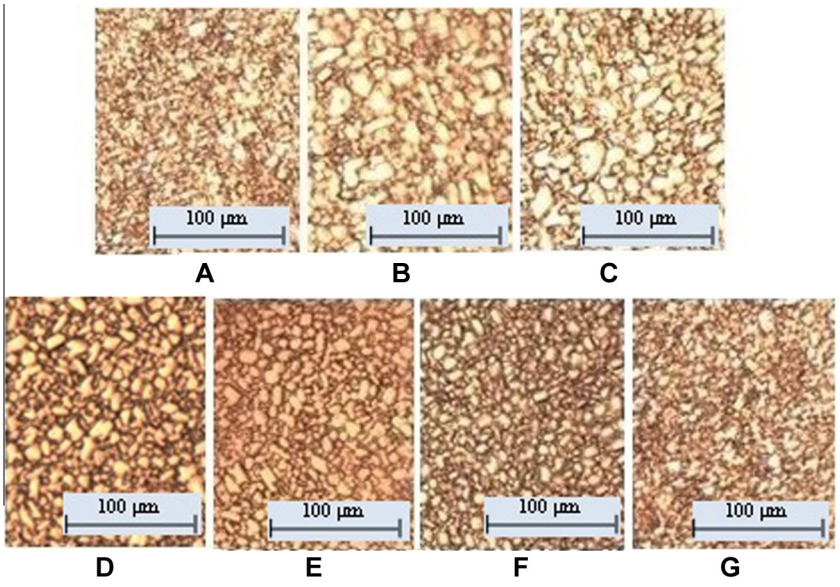

H

	Concentration (%, w/v)	T_g (°C)
a		-31.69±1.22
b	0.5	-29.93±2.04
c	0.05	-29.34±1.08
d	0.1	-28.14±2.11
e	0.2	-25.71±1.76
f	0.3	-22.79±1.65
g	0.5	-17.64±2.01

Fig. 5. Effect of AP-3 ice-binding collagen peptides on crystal growth and T_g in ice cream mix. (A) Control ice cream at −16 °C, (B) control ice cream after seven cycles at −16 to −14 °C and (C–G) ice cream + AP-3 ice-binding collagen peptides at 0.05%, 0.1%, 0.2%, 0.3% and 0.5% after seven cycles at −16 to −14 °C. (H) Effects of AP-3 ice-binding collagen peptides on the T_g of ice cream (a, blank; b, ice cream + 0.5% BSA; c–g, ice cream + 0.05–5% AP-3 ice-binding collagen peptide).

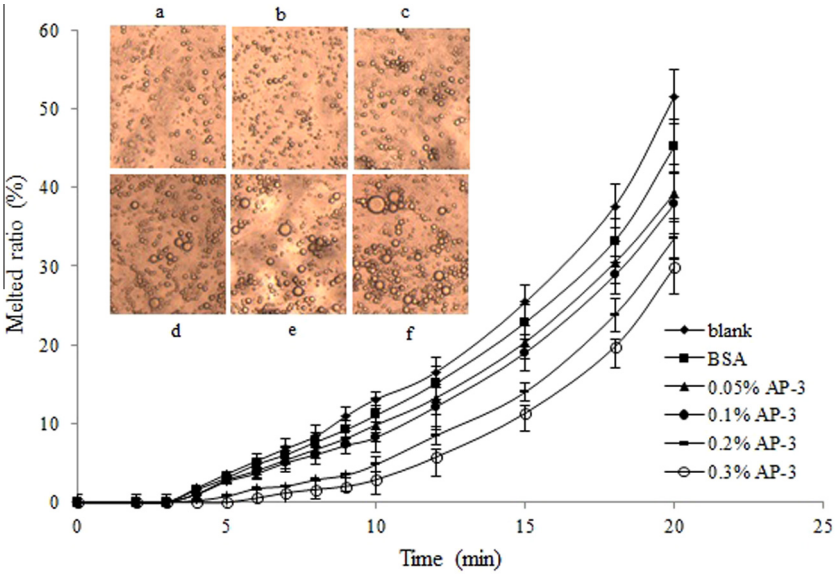

Fig. 6. Effects of AP-3 ice-binding collagen peptide at different concentrations on the melting ratio of ice cream; (inset) effects of blank (a), BSA (b), AP-3 0.05% (c), AP-3 0.1% (d), AP-3 0.2% (e) and AP-3 0.3% (f) on air bubbles in ice cream.

and the melting rate was the lowest of all samples. It can also be seen that ice cream with 0.2% or 0.3% AP-3 showed a relatively regular and larger air bubble distribution compared to other ice cream samples (Fig. 6 inset).

Increasing AP-3 ice-binding collagen peptide concentrations enhanced the melt-resistance of ice cream by decreasing ice crystal size. Thus, more time will be needed for water to flow through the complex foamy structure of the ice cream resulted by smaller ice crystals. In addition, the high melt-resistance of ice creams with added AP-3 may be related to low heat transfer rates. Larger air cells inhibit heat transfer, resulting in low melting rates.

4. Conclusion

Antifreeze proteins share two related abilities: to depress the freezing temperature below the melting point of ice and to inhibit the restructuring of ice into larger crystals. In this study, we isolated and characterised a novel ice-binding collagen peptide from purified porcine collagen. The results indicated that the AP-3 ice-binding collagen peptide (GLLGPLGPRGLL) with 1162.8 Da molecular weights exhibited the highest TH (5.28 °C), which can be classified as "hyperactive". Recrystallisation, melt-resistance and glass transition temperature of ice cream was also improved by AP-3 ice-binding collagen peptide. These findings suggested that AP-3 ice-binding peptide is a novel antifreeze molecule derived from collagen, which exhibits a strong ice-binding activity, could be used as a beneficial additive to probiotics or other processed foods that require low temperature storage.

Compliance with ethics requirements

This article does not contain any studies with human or animal subjects.

Conflict of interest

None declared.

Acknowledgments

This work was financially supported by the National High Technology Research and Development Program of China (863 Program, No. 2013AA102207), the National Natural Science Funds (Nos. 31201421, 31101283).

References

Adler-Nissen, J. (1986). *Enzymatic hydrolysis of food proteins*. New York, USA: Elsevier Applied Science Publishers Ltd.

Baardsnes, J., & Davies, P. L. (2002). Contribution of hydrophobic residues to ice binding by fish type III antifreeze protein. *Biochimica Et Biophysica Acta-Proteins and Proteomics, 1601*, 49–54.

Bravo, L. A., & Griffith, M. (2005). Characterization of antifreeze activity in Antarctic plants. *Journal of Experimental Botany, 56*, 1189–1196.

Burcham, T. S., Osuga, D. T., Yeh, Y., & Feeney, R. E. (1986). A kinetic description of antifreeze glycoprotein activity. *Journal of Biological Chemistry, 261*, 6390–6397.

Chao, H., Houston, M. E., Hodges, R. S., Kay, C. M., Sykes, B. D., & Loewen, M. C. (1997). A diminished role for hydrogen bonds in antifreeze protein binding to ice. *Biochemistry, 36*, 14652–14660.

Damodaran, S. (2007). Inhibition of ice crystal growth in ice cream mix by gelatin hydrolysate. *Journal of Agricultural and Food Chemistry, 55*, 10918–10923.

Desjardins, M., Le Francois, N. R., Fletcher, G. L., & Blier, P. U. (2007). High antifreeze protein levels in wolffish (*Anarhichas lupus*) make them an ideal candidate for culture in cold, potentially ice laden waters. *Aquaculture, 272*, 667–674.

DeVries, A. L., & Wohlschlag, D. E. (1969). Freezing resistance in some Antarctic fishes. *Science, 163*, 1073–1075.

Ding, X., Zhang, H., Liu, W., Wang, L., Qian, F., & Qi, X. (2014). Extraction of carrot (*Daucus carota*) antifreeze proteins and evaluation of their effects on frozen white salted noodle. *Food and Bioprocess Technology, 7*, 842–852.

Duman, J. G., Bennett, V., Sformo, T., Hochstrasser, R., & Barnes, B. M. (2004). Antifreeze proteins in Alaskan insects and spiders. *Journal of Insect Physiology, 50*, 259–266.

Fletcher, G. L., Hew, C. L., & Davies, P. L. (2001). Antifreeze proteins of teleost fishes. *Annual Review of Physiology, 63*, 359–390.

Gelse, K., Poschl, E., & Aigner, T. (2003). Collagens-structure, function, and biosynthesis. *Advanced Drug Delivery Reviews, 55*, 1531–1546.

Gilbert, J. A., Hill, P. J., Dodd, C. E. R., & Laybourn-Parry, J. (2004). Demonstration of antifreeze protein activity in Antarctic lake bacteria. *Microbiology, 150*, 171–180.

Graham, L. A., & Davies, P. L. (2005). Glycine-rich antifreeze proteins from snow fleas. *Science, 310*, 461–465.

Graether, S. P., & Sykes, B. D. (2004). Cold survival in freeze-tolerant insects. *European Journal of Biochemistry, 271*, 3285–3296.

Hansen, T. N., & Baust, J. G. (1988). Differential scanning calorimetric analysis of antifreeze protein activity in the common mealworm, *Tenebrio molitor*. *Biochimica et Biophysica Acta, 957*, 217–221.

Holt, C. B. (2003). Substances which inhibit ice nucleation: A review. *Cryo Letters, 24*, 269–274.

Kristiansen, E., & Zachariassen, K. E. (2008). The mechanism by which fish antifreeze proteins cause thermal hysteresis. *Cryobiology, 51*, 262–280.

Li, Z., Marshall, R., Heymann, H., & Fernando, L. (1997). Effects of milk fat content on flavor perception of vanilla ice cream. *Journal of Dairy Science, 80*, 3133–3141.

Lin, F. H., Graham, L. A., Campbell, R. L., & Davies, P. L. (2007). Structural modeling of snow flea antifreeze protein. *Biophysical Journal, 92*, 1717–1723.

Lu, M., Wang, B., Li, Z., Fei, Y., Wei, L., & Gao, S. (2002). Differential scanning calorimetric and circular dichroistic studies on plant antifreeze proteins. *Journal of Thermal Analysis and Calorimetry, 67*, 689–698.

Muse, M., & Hartel, R. (2004). Ice cream structural elements that affect melting rate and hardness. *Journal of Dairy Science, 87*, 1–10.

Nagai, T., & Suzuki, N. (2000). Isolation of collagen from fish waste material – skin, bone and fins. *Food Chemistry, 68*, 277–281.

Pertaya, N., Marshall, C. B., Celik, Y., Davies, P. L., & Braslavsky, I. (2008). Direct visualization of spruce budworm antifreeze protein interacting with ice crystals: Basal plane affinity confers hyperactivity. *Biophysical Journal, 95*, 333–341.

Ramlov, H., DeVries, A. L., & Wilson, P. W. (2005). Antifreeze glycoproteins from the Antarctic fish Dissostichus mawsoni studied by differential scanning calorimetry (DSC) in combination with nanolitre osmometry. *Cryo Letters, 26*, 73–84.

Raymond, J. A., & DeVries, A. L. (1977). Adsorption inhibition as a mechanism of freezing resistance in polar fishes. *Proceedings of the National Academy of Sciences, 74*, 2589–2593.

Regand, A., & Goff, H. D. (2002). Effects of biopolymers on structure and ice recrystallization in dynamically-frozen ice cream model systems. *Journal of Dairy Science, 85*, 2722–2732.

Scotter, A. J., Marshall, C. B., Graham, L. A., Gilbert, J. A., Garnham, C. P., & Davies, P. L. (2006). The basis for hyperactivity of antifreeze proteins. *Cryobiology, 53*, 229–239.

Shih, F. F., & Daigle, K. W. (2000). Preparation and characterization of rice protein isolates. *Journal of the American Oil Chemists Society, 77*, 885–889.

Tachibana, Y., Fletcher, G. L., Fujitani, N., Tsuda, S., Monde, K., & Nishimura, S. I. (2004). Antifreeze glycoproteins: Elucidation of the structural motifs that are essential for antifreeze activity. *Angewandte Chemie-International Edition, 43*, 856–862.

Wang, S. Y., Agyare, K., & Damodaran, S. (2009). Optimisation of hydrolysis conditions and fractionation of peptide cryoprotectants from gelatin hydrolysate. *Food Chemistry, 115*, 620–630.

Wang, S. Y., & Damodaran, S. (2009). Ice-structure peptides derived from bovine collagen. *Journal of Agricultural and Food Chemistry, 57*, 5501–5509.

Wang, S. Y., Zhao, J., Chen, L., Zhou, Y. F., & Wu, J. H. (2014). Preparation, isolation and hypothermia protection activity of antifreeze peptides from shark skin collagen. *LWT-Food science and technology, 55*, 210–217.

Wu, J. H., Rong, Y. Z., Wang, Z. W., Zhou, Y. F., Wang, S. Y., & Zhao, B. (2015). Isolation and characterization of sericin antifreeze peptides and molecular dynamics modeling of their ice-binding interaction. *Food Chemistry, 174*, 621–629.

Wen, D., & Laursen, R. A. (1992). Structure-function relationships in an antifreeze polypeptide. The role of neutral, polar amino acids. *Journal of Biological Chemistry, 267*, 14102–14108.

Wisniewski, M., Webb, R., Balsamo, R., Close, T. J., Yu, X. M., & Griffith, M. (1999). Purification, immunolocalization, cryoprotective and antifreeze activity of bPCA60: A dehydrin from peach (Prunuspersica). *Plant Physiology, 105*, 600–608.

Worrall, D., Elias, L., Ashford, D., Smallwood, M., Sidebottom, C., Lillford, P., et al. (1998). A carrot leucine-rich repeat protein that inhibits ice recrystallization. *Science, 282*, 11–13.

Wua, Y., Banoubb, J., Goddarda, S. V., Kao, M. H., & Fletcher, G. L. (2001). Antifreeze glycoproteins: Relationship between molecular weight, thermal hysteresis and the inhibition of leakage from liposomes during thermotropic phase transition. *Comparative Biochemistry and Physiology Part B, 128*, 265–273.

Yeh, Y., & Feeney, R. E. (1996). Antifreeze proteins: Structures and mechanisms of function. *Chemical Reviews, 96*, 601–617.